Monthly Notices
of the
ROYAL ASTRONOMICAL SOCIETY

MNRAS **449,** 1811–1818 (2015) doi:10.1093/mnras/stv395

Evidence of tidal distortions and mass-loss from the old open cluster NGC 6791

E. Dalessandro,[1]⋆ P. Miocchi,[1] G. Carraro,[2] L. Jílková[3] and A. Moitinho[4]

[1]*Dipartimento di Astronomia, Università degli Studi di Bologna, via Ranzani 1, I-40127 Bologna, Italy*
[2]*ESO, Alonso de Cordova 3107, 19001 Santiago de Chile, Chile*
[3]*Leiden Observatory, PO Box 9513, NL-2300 RA Leiden, the Netherlands*
[4]*SIM/CENTRA, Faculdade de Ciencias de Universidade de Lisboa, Ed. C8, Campo Grande, P-1749-016 Lisboa, Portugal*

Accepted 2015 February 20. Received 2015 February 19; in original form 2015 January 13

ABSTRACT

We present the first evidence of clear signatures of tidal distortions in the density distribution of the fascinating open cluster NGC 6791. We used deep and wide-field data obtained with the Canada–France–Hawaii Telescope covering a $2^\circ \times 2^\circ$ area around the cluster. The 2D density map obtained with the optimal matched filter technique shows a clear elongation and an irregular distribution starting from ∼300 arcsec from the cluster centre. At larger distances, two tails extending in opposite directions beyond the tidal radius are also visible. These features are aligned to both the absolute proper motion and to the Galactic Centre directions. Moreover, other overdensities appear to be stretched in a direction perpendicular to the Galactic plane. Accordingly to the behaviour observed in the density map, we find that both the surface brightness and the star count density profiles reveal a departure from a King model starting from ∼600 arcsec from the centre. These observational evidence suggest that NGC 6791 is currently experiencing mass-loss likely due to gravitational shocking and interactions with the tidal field. We use this evidence to argue that NGC 6791 should have lost a significant fraction of its original mass. A larger initial mass would in fact explain why the cluster survived so long. Using available recipes based on analytic studies and *N*-body simulations, we derived the expected mass-loss due to stellar evolution and tidal interactions and estimated the initial cluster mass to be $M_{\rm ini} = (1.5\text{–}4) \times 10^5\,{\rm M}_\odot$.

Key words: stars: evolution – stars: imaging – open clusters and associations: individual: NGC 6791.

1 INTRODUCTION

NGC 6791 is one of the most intriguing open cluster (OC) in the Galaxy. It possesses a unique set of properties that have attracted a lot of attention in the last decade.

Indeed, NGC 6791 is one of the most massive ($M \sim 5000\,{\rm M}_\odot$; Platais et al. 2011), oldest ($t \sim 8$ Gyr; King et al. 2005; Grundahl et al. 2008; García-Berro et al. 2010; Brogaard et al. 2012) and most metal-rich ([Fe/H] ∼ +0.40; Carraro et al. 2006; Gratton et al. 2006; Origlia et al. 2006) Galactic OCs. More specifically, this combination of properties is unique for clusters at its Galactocentric distance ($d \sim 8$ Kpc; Carraro 2014). Stars with similar age and metallicity are found in the Galactic bulge (Bensby et al. 2013) where it has been suggested (Jílková et al. 2012) NGC 6791 might have formed.

Given its peculiarities, and in particular its mass, NGC 6791 represents an ideal link between OCs and globular clusters. For this reason, it has been widely targeted to understand whether star-to-star variations of light element (C, N, O, Na, O, Mg and Al) abundances can be found also in this system as observed in basically all globular clusters (Gratton et al. 2012). This topic is still matter of debate and no consensus has been reached so far on whether the cluster hosts more than one generation of stars. Geisler et al. (2012) presented evidence of Na–O anticorrelation among giant stars in NGC 6791, while recently Bragaglia et al. (2014) and Cunha et al. (2015) have questioned this result finding an homogeneous Na abundance (within ∼0.1 dex).

NGC 6791 shows also an anomalous horizontal branch (HB) with a well-populated red clump, as expected for its high metallicity, and a group of hot HB stars (Liebert, Saffer & Green 1994; Tofflemire et al. 2014), whose origin is still not completely understood (Carraro 2014). The combined UV flux of the few hot HB stars and its metallicity makes this cluster a fairly good proxy of standard UV-upturn elliptical galaxies (Buzzoni et al. 2012). This result is supported also by the Lick indices analysis of its spectral energy distribution.

This plethora of unique properties makes NGC 6791 an extremely interesting object to study and understand. A number of questions

⋆ E-mail: emanuele.dalessandr2@unibo.it

about the nature of this system still arise: how and where could such a stellar system have formed? Is NGC 6791 a genuine OC? Did it form close to the bulge? How could have survived for so long in the adverse high-density environment of the inner Galactic disc, where it presently is? One of the still missing key ingredient that could help to understand the origin of such a fascinating system is its original mass.

The mass budget of any stellar system is strongly affected by two-body relaxation, stellar evolution, encounters with giant molecular clouds and spiral arms, interactions with the tidal field. The disruption scenarios and the survival rates of Galactic OCs have been studied since the 1960s (Spitzer 1958; Spitzer & Harm 1958). Recently, *N*-body simulations (e.g. Gieles et al. 2006; Gieles & Baumgardt 2008) have also shown the impact of giant molecular clouds and of the initial structure of OCs on their dissolution. The OC orbits have generally small eccentricities and they tend to be located at a small height (Z) on the Galactic plane, as a consequence they are expected to pass many times through the Galactic disc. Each of these gravitational shocks heat up and compress the cluster which then takes an elongate shape which flattens to its maximum at $Z = 0$ (Leon 1998). Repeated disc-shocking speed-up the disruption of OCs (Combes, Leon & Meylan 1999) and after each passage cluster stars rejected in the halo of the system are stripped out by the gravitational field of the Galaxy. These ejected stars are expected to form tidal tails extending far from the cluster inner regions. Indeed, Davenport & Sandquist (2010) and Bergond, Leon & Guibert (2001) have found that some OCs show a quite elongated and extended structures likely resulting from the interactions with the Galactic tidal field.

In general, OCs are thought to dissipate in a time-scale of the order of $\sim 10^7$–10^8 yr (Binney & Tremaine 1987). In this context, the existence of very old OCs like NGC 6791 represents an anomaly.[1] This system may have managed to survive so long either because it moved along a preferential orbit or its original mass was much larger than observed today.

In this paper, we analyse the two-dimensional (2D) and projected density distributions of NGC 6791 with the aim of understanding whether the cluster suffered from strong tidal interactions that could have significantly decreased its mass. We find that this system has an elongated structure and shows overdensities in the external regions that are aligned to the direction of the orbital motion. These features strongly suggest that this system has likely lost part of its mass because of gravitational shocks and interaction with the Galactic tidal field. We use this argument to support the hypothesis that this system was significantly more massive than observed today and we derive an estimate for its original mass by means of a simplified analytic approach.

The paper is organized as follows: in Section 2, data set and data-reduction procedures are described, in Section 3 the 2D density map is obtained while in Section 4 both the star-count projected density and the surface brightness profiles are analysed; finally in Section 5 we estimate, the initial mass of NGC 6791.

2 OBSERVATIONS AND DATA REDUCTION

We used deep proprietary images (Prop ID: OPTICON 2013B/005; PI Moitinho) obtained with the wide field imager MegaCam mounted at the Canada–France–Hawaii Telescope (CFHT). This camera consists of a mosaic of 36 chips of 2048 × 4612 pixels each, with a pixel scale of 0.185 arcsec pixel^{-1} providing a total field of view of $\sim 1^\circ \times 1^\circ$. We used four different pointings set up to cover a total field of view of $\sim 2^\circ \times 2^\circ$ centred approximately on the cluster centre (Fig. 1). For each pointing, four images acquired both with the g' and r' bands and with exposure times $t_{\rm exp} = 100$ and 180 s, respectively, have been secured. An appropriate dither pattern of few arcsec has been adopted for each pointing. This allowed us to cover most of the interchip gaps, with the exception of the most prominent and horizontal ones (see Fig. 1).

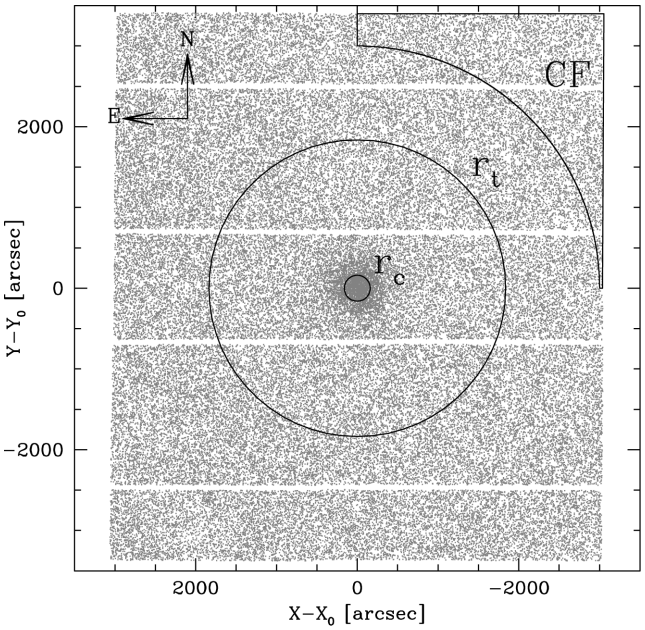

Figure 1. Map of the entire CFHT data base with respect to the position of $C_{\rm grav}$ (X_0, Y_0). The two circles represent the location of core ($r_{\rm c}$) and tidal radii ($r_{\rm t}$). The box in the upper-right corner defines the 'control field' (CF) area.

The data were pre-processed (i.e. bias and flat-field corrected) by the Elixir pipeline developed by the CFHT team. By means of an iterative procedure, an adequate number (>20) of isolated and bright stars have been selected in each chip and band to model the point spread function (PSF). Then, the PSF model was applied to all the stellar-like sources at about 4σ from the local background by using DAOPHOT and the PSF-fitting algorithm ALLSTAR (Stetson 1987). For each filter and chip, we matched the single-frame catalogues to obtain a master list. Finally, the g' and r' master lists were then geometrically matched and combined. Each master list includes the instrumental magnitude, defined as the weighted mean of the single image measurement reported to the system reference frame of the transformation, and the error, which is the standard error of the mean.

The instrumental coordinates have been reported independently for each chip to the absolute astrometric system (α, δ) using a large number of stars in common with the DR7 release of the Sloan Digital Sky Survey (Abazajian et al. 2009) and following the procedure described by Dalessandro et al. (2009). Using the same stars, we derived for each chip and band the zero-points to report the instrumental magnitudes to the Sloan photometric system. At this stage all the master lists are in the same photometric and astrometric system. We then merged them to create the final catalogue, which counts about 270 000 stars.

The $(g', g' - r')$ colour–magnitude diagrams (CMDs) of NGC 6791 and of the surrounding field are shown in Fig. 2. In the CMDs,

[1] Other old (t > 2–3 Gyr) OCs for which such an argument applies are NGC 188, M67 and Berkley 11.

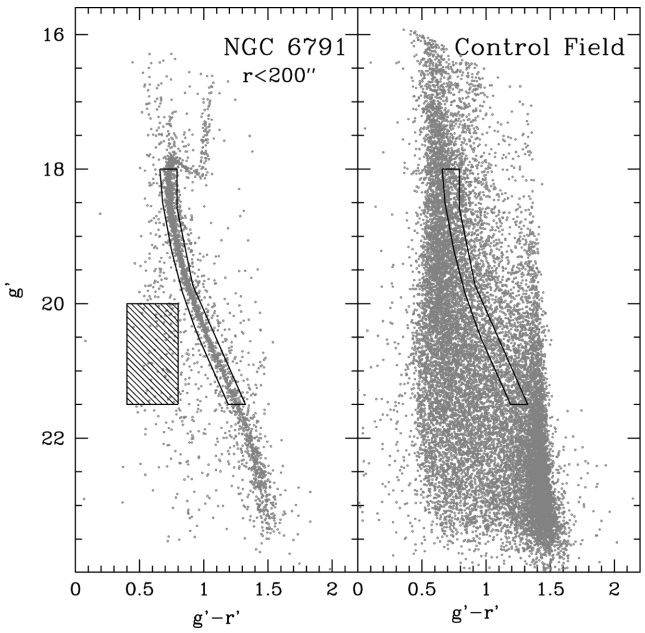

Figure 2. $(g', g' - r')$ CMDs of the innermost region of NGC 6791 (left-hand panel) and of the control field' (right-hand panel). The black box along the MS of NGC 6791 encloses the region in the CMD where CP stars have been selected. The shaded area defines the region where fiducial Galactic disc MS stars have been selected.

it is possible to clearly distinguish the main sequence (MS) of the cluster (left-hand panel of Fig. 2), extending down to $g' \sim 23.5$ in the innermost regions, corresponding to about five magnitudes below the turn-off. Also, it is possible to note that our data suffer of strong saturation starting at $g' \sim 17$. Two almost vertical sequences located around $(g' - r') \sim 0.6$ and $(g' - r') \sim 1.5$ are clearly visible both in the innermost (Fig. 2 left-hand panel) and external regions (Fig. 2 right-hand panel). They are populated by M-dwarf and MS Galactic disc stars.

A differential reddening of about $\Delta E(B - V) \sim 0.05$ has been estimated for this cluster (see for example Platais et al. 2011). Indeed, at the level of the turn-off ($g' \sim 18$), the MS shows a mild broadening not explainable in terms of pure photometric errors. Such an effect disappears at fainter magnitudes ($g' \sim 19$), where the MS starts to bend diagonally in the $(g', g' - r')$ CMD. Given its relatively small amplitude, we will neglect the effect of differential reddening in the following analysis.

3 THE DENSITY MAP

3.1 The matched filter analysis

To probe the spatial distribution of NGC 6791, we first analysed the 2D density distribution.

The density analysis of NGC 6791 has been performed in the circular area enclosed within a distance from the cluster centre (see details in Section 4) $r = 3000$ arcsec, thus covering a $1.^{\circ}7 \times 1.^{\circ}7$ area. We selected stars along the MS in the magnitude range $18 < g' < 21.5$ and within three times the local colour dispersion about the cluster mean ridge line (see Fig. 2). Stars selected in this way define the 'cluster population' (CP) sample. These selection criteria have been chosen to ensure a good level of completeness and to minimize the contamination from Galactic field stars. Variations of the adopted magnitude limits do not affect the final result.

As a first qualitative step, we obtained a rough smoothed density distribution of CP stars. As expected, at a first look, the distribution of CP stars appears to be extremely concentrated around the position of the cluster and it shows some irregularities and structures allover the field of view (FOV). We also note that the north-west quadrant shows on average a smoother distribution than the other quadrants for $r > 1000$ arcsec.

To investigate in more detail the 2D distribution of CP stars, we adopted the widely used optimal matched filter technique (see for example Kuhn, Smith & Hawley 1996; Odenkirchen et al. 2001, 2003; Rockosi et al. 2002). It has been shown (Davenport & Sandquist 2010) that this method is robust for identifying low-density stellar populations against a significant background, as in the case of OCs. The optimal matched filter technique requires to use a fiducial field population as reference. For this purpose, we selected stars in the same magnitude and colour bins as the CP sample and located at $r > 3000$ arcsec from the cluster centre in the north-west quadrant (because of its apparent homogeneous distribution). We named this sample of stars 'control field' (CF; Figs 1 and 2).

We computed the densities in the CMDs (Hess diagrams) of both the CP and CF samples. Then we assigned to each star in the CP sample a weight defined as the reciprocal of the fraction of CF stars lying within a fixed range of colour and magnitude from its location in the CMD.

Finally, the weighted distribution of star positions was transformed into a smoothed surface density function through the use of a kernel whose width has been chosen to be large enough so as to make negligible the impact of the gaps in the FOV. This procedure yields the surface density distribution shown in Fig. 3. As apparent, the overall density distribution is elongated and irregular. In particular, we observe that the innermost ∼300 arcsec are quite spherical, while at larger distance the cluster starts to be distorted mainly along the north-east/south-west direction in an almost symmetrical way respect to the centre of the cluster. At $r > 1000$ arcsec, two tails running at opposite directions are clearly visible, with the one in the southern direction extending up to distances larger than 2500 arcsec from the cluster centre. It is important to note that both the external tidal arms and the innermost elongation of the cluster run almost parallel to the absolute proper motion vector (Bedin et al. 2006) and to the direction of the Galactic Centre (GalC; Fig. 3). This behaviour is in agreement with a real tidal nature for the observed distortions. In fact, the orbital motion of NGC 6791 likely develops close to the Galactic equatorial plane (Jílková et al. 2012) and, since tidal tails are supposed to lie on the orbital plane (at least in axisymmetric potentials; see Montuori et al. 2007), they are expected to be seen with such a projected alignment. Moreover, other distortions extending almost perpendicularly to the PM direction are clearly visible and their formation could be related to the tidal effect due to the Galactic disc (e.g. Bergond et al. 2001).

The features observed in the 2D density distribution of NGC 6791 are indeed typical evidence of recent stellar mass-loss due to dynamical evolution of the system under the tidal influence of the overall Galactic potential. It is interesting to note that the density map of NGC 6791 is qualitatively similar to that observed in M67 by Davenport & Sandquist (2010) and to a weaker extent to other three OCs (namely NGC 2287, NGC 2516 and NGC 2548) by Bergond et al. (2001).

We also note that in the south-east quadrant for $r > 2000$ arcsec there is a star density increase that does not seem to be directly connected to the cluster. Interestingly enough, this overdensity appears at decreasing Galactic latitude; therefore, we speculate that it might be due to the density gradient of Galactic disc stars.

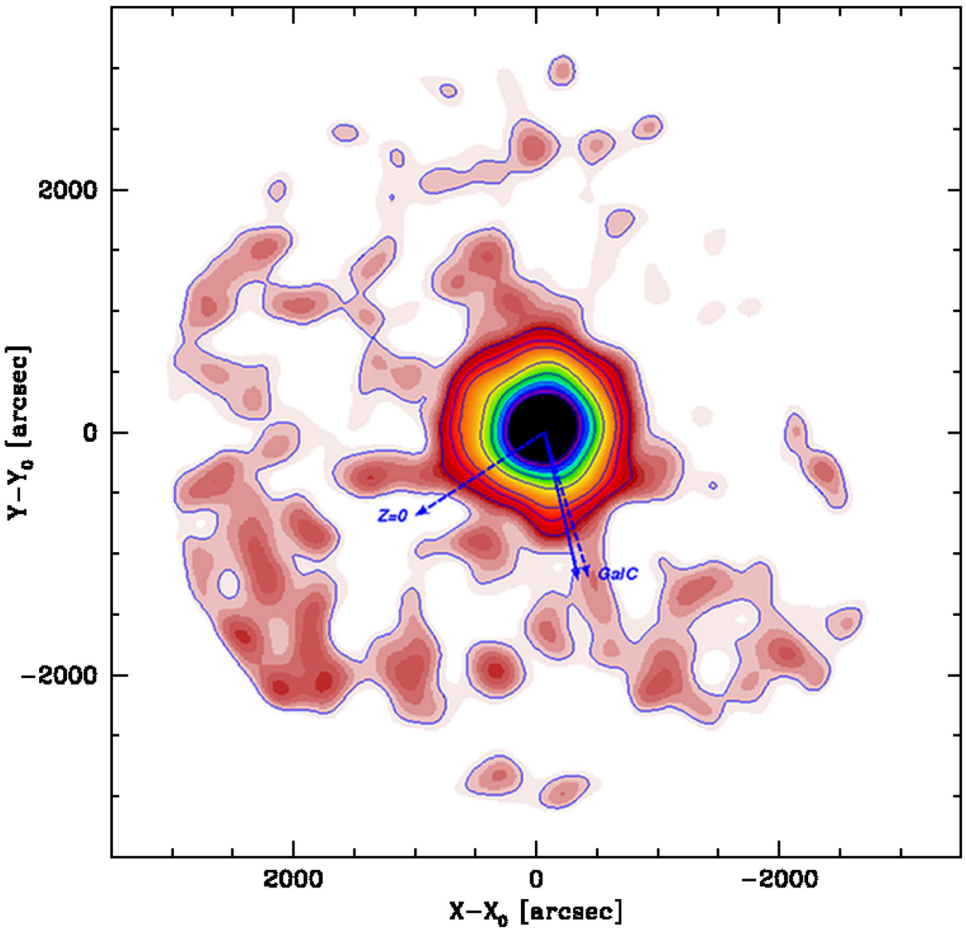

Figure 3. Large-scale 2D colour-coded surface density map around NGC 6791. The contour levels span from 3σ to 40σ with irregular steps. The solid arrow represents the direction of the absolute proper motion of NGC 6791, while the dashed ones mark the direction of the Galactic Centre (GalC) and that perpendicular to the Galactic plane ($Z = 0$).

3.2 Sanity checks

To further check the significance of the anisotropic distribution of NGC 6791, we used for comparison stars selected in the CMD in the range $0.4 < (g' - r') < 0.8$ and $20 < g' < 21.5$ (see Fig. 2). These are likely MS Galactic disc stars and they trace the behaviour of the main contributors to the contamination of CP stars. This sample is supposed to be homogeneously distributed across the FOV and actual deviations from a smooth distribution reflect variations in the detection efficiency, Galactic field and/or extinction gradients.

We performed on this subsample the same analysis done previously for CP stars. The 2D density map of MS Galactic disc stars is shown in Fig. 4. We observe that in general they are uniformly distributed across the FOV as expected, but they show a density excess in the external regions of the south-east quadrant. This evidence further suggests that the relevant feature in the 2D density distribution of CP stars at $r > 2000$ arcsec (Fig. 3) in this quadrant, is likely due to a gradient of the density of the Galactic disc within the FOV.

In addition, we divided the FOV in 10 angular sectors of 36° each with vertex at the cluster centre. Then, for each sector with angle θ measured counterclockwise from the west direction, and for different distances from the cluster centre, we estimated the ratio between CP stars ($N_{\rm CP}$), and likely Galactic disc MS stars, selected as described before ($N_{\rm field}$). The results for $r < 500$ arcsec

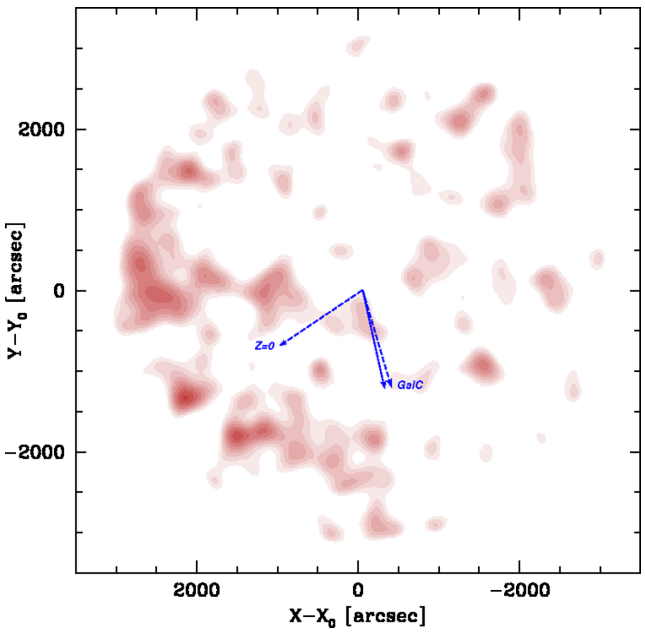

Figure 4. As in Fig. 3, but for stars with $0.4 < (g' - r') < 0.8$ and $20 < g' < 21.5$, which are representative of the Galactic field contamination (see Section 3.2). Colours are in the same relative scale as in Fig. 3.

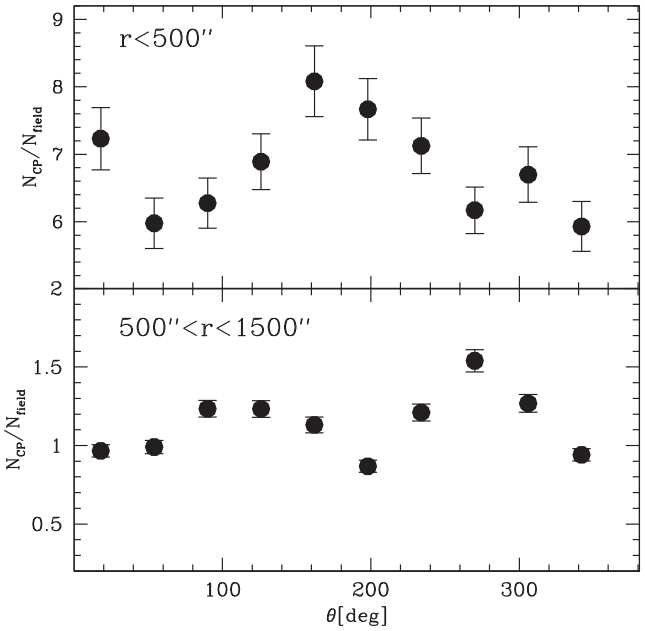

Figure 5. Ratio between CP and field stars as a function of the position angle θ (Section 3) for stars at $r < 500$ arcsec (upper panel) and at 500 arcsec $< r <$ 1500 arcsec (lower panel).

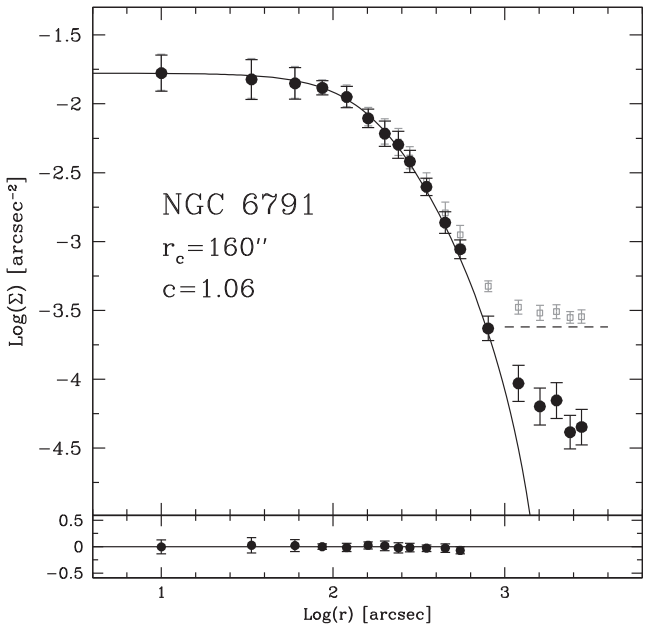

Figure 6. Observed star count density profile as a function of radius (open grey squares). The dashed line represents the density value of the background as obtained by averaging the four outermost density measurements in the north-west quadrant. The black filled dots are densities obtained after background subtraction. The best single-mass King model is also overplotted to the observations (solid line) and the structural parameters are labelled. The lower panel shows the residual between the observations and the best-fitting model.

and 500 arcsec $< r <$ 1500 arcsec are shown in Fig. 5. In both cases, the ratio shows significant variations as a function of θ, as expected for a real anisotropic density distribution. Moreover, it is also worth noting that different patterns in the central and outermost regions appear. For 500 arcsec $< r <$ 1500 arcsec, the maxima of the ratio occur at $\theta = 100^\circ$ and $\theta = 280^\circ$ corresponding to the two opposite main tidal arms.

These sanity checks demonstrate that the observed 2D density distribution shown in Fig. 3 is a real feature of NGC 6791 and cannot be ascribed to observational bias or field gradients.

4 STAR DENSITY AND SURFACE BRIGHTNESS PROFILES

Star density distortions, elongation and tidal tails are expected to be detected also in the radial density profile (see for example Odenkirchen et al. 2003; Capuzzo-Dolcetta, Di Matteo & Miocchi 2005). Therefore as a second step of our analysis, we studied the projected density profile of NGC 6791.

First, we derived the centre of gravity ($C_{\rm grav}$) by using an iterative procedure (see for example Dalessandro et al. 2013) and averaging the positions α and δ of CP stars. We used the centre reported by the WEBDA web page[2] as starting guess point of our procedure. To avoid spurious effects due to incompleteness, we performed several estimates by adopting different magnitude and distance selections. In particular, we used three different magnitude bins in the range $18 < g' < 21.5$, with the upper limit (fainter magnitude) increasing by 0.5 mag at each step. For each magnitude bin, we repeated the procedure for four different radial selections, from 250 to 400 arcsec with a step of 50 arcsec. We ended up with a total of 20 estimates. The resulting $C_{\rm grav}$ is the average of these measures and it is located at $\alpha_c = 19^{\rm h}20^{\rm m}54\overset{\rm s}{.}273$ and $\delta_c = 37^\circ46'25\overset{''}{.}20$ (RA= 290.226 1395 Dec. = 37.773 667 12), with an uncertainty of ∼1.2 arcsec. This new determination is located at ∼12 arcsec north-east from the centre reported by the WEBDA web page. While it is not trivial to understand the origin of this discrepancy, we stress here that it has a negligible impact on the results presented in this paper.

The projected density profile of NGC 6791 has been determined using direct counts of CP stars. We excluded the south-east quadrant from the analysis since in the most external part of this region the star distribution is dominated by MS Galactic disc stars (Section 3.1). Using the procedure described in Dalessandro et al. (2013), we divided the considered FOV into 18 concentric annuli, each centred on $C_{\rm grav}$ and suitably split in an adequate number of subsectors. Number counts have been calculated in each subsector and the corresponding densities were obtained dividing them by the sampled area. Incomplete area coverage, mainly due to the presence of gaps (Fig. 1), have been properly taken into account. The stellar density of each annulus was then defined as the average of the subsector densities and its standard deviation computed from the variance among the subsectors. The resulting projected surface density profile is shown in Fig. 6.

We estimated the background density contribution by using only stars in the north-west quadrant. In fact, as discussed before (see also Fig. 3) this region is free by any evident structure caused either by the cluster elongation or from field stars. The background contribution has been estimated as the average of the four outermost density measurements ($r > 1400$ arcsec), which define a kind of plateau at $\log(\rho_{\rm bck}) \sim -3.6$ stars arcsec^{-2}. We then subtracted this value to the observed density profile. We have verified that this choice is appropriate. In fact, the contribution to the background due to field stars (see selection criteria in Section 3.1) is constant in all quadrants but the south-east one.

[2] http://www.univie.ac.at/webda/cgi-bin/ocl_page.cgi?dirname=ngc6791

The derived density profile has been reproduced by using a single-mass King model (King 1966). The fitting procedure is fully described in Miocchi et al. (2013). The fit was limited to the innermost $r < 500$ arcsec to avoid the most elongated regions of the cluster. The best fit is obtained for a concentration $c = 1.06$ (corresponding to a central dimensionless potential $W_0 = 5.3$) and core radius $r_c = 160$ arcsec. These parameters are in partial disagreement with those obtained by Platais et al. (2011, $c = 0.74$, $r_c = 196$ arcsec) which to our knowledge is the only other density profile analysis present in the literature for NGC 6791. The authors obtained the density profile using stars with $g' < 22$ and weighted according to their proper motion. However, their data were limited to the innermost 900 arcsec and therefore the determination of the tidal radius and any residual in the background contribution was rather unstable.

As apparent in Fig. 6, for $\log(r) > 2.8$ ($r > 600$ arcsec) the density profile clearly deviates from the behaviour predicted by the King model. The use of a Wilson model (Wilson 1975) does not provide any significant improvement on the overall quality of the fit. We have also checked that even if we do not constrain the model to fit the innermost region, there is no way to satisfactory reproduce the density profile for $r > 600$ arcsec. The external part of the projected density profile instead follows a power-law behaviour with an exponent $\alpha \sim -1.7$, in agreement with the values found in Galactic globular clusters with observed tidal tails (see for example Sollima et al. 2011 and references therein) and as predicted by theoretical models (Johnston et al. 1999). Küpper et al. (2010) analysed the variation of the power-law slopes of tidal tails of dissolving clusters as a function of the orbital phase, eccentricity and initial cluster densities by means of *N*-body simulations. They found that the power-law slopes have typical values $\alpha = -5$ that can increase reaching values $\alpha \sim -2$ for systems with highly eccentric orbits and close to or at the apogalacticon, where tidal tails get strongly compressed. This upper limit is in good agreement with what found for NGC 6791; however, we should note that the analysis by Küpper et al. (2010) is performed on clusters moving on orbits perpendicular to the line of sight, while this is not the case for NGC 6791. As a consequence the relatively shallow power law observed in NGC 6791 can be the result also of projection effects.

To further investigate the results just described and check whether they might be caused by incompleteness or bias of our photometric catalogue, we also derived the surface brightness profile by performing the analysis directly on FITS images (see for example Dalessandro et al. 2012). We used a low-resolution single-plate ESO Digitalized Sky Survey image obtained in optical band and extending up to about 2000 arcsec from C_{grav}. We limited the analysis to the same quadrants used for deriving the star counts density profile and we used the north-west quadrant to estimate the background contribution. We divided the FOV in a similar number of concentric annuli and subsectors. The surface brightness assigned to each annulus is given by the ratio between the mean of the fluxes measured in the subsectors and the area covered by the annulus. The resulting surface brightness profile is shown in Fig. 7. First, we observe that the King model best fit the star counts density profile well reproduces also the surface brightness profile. More importantly, we note that consistently with what found in the star count projected density profile, for $r > 600$ arcsec the surface brightness profile starts to deviate from the behaviour predicted by the model and it declines as a power law.

We can therefore safely conclude that both the 2D density map and the density (surface brightness) profile analysis suggest that NGC 6791 is currently experiencing tidal stripping events.

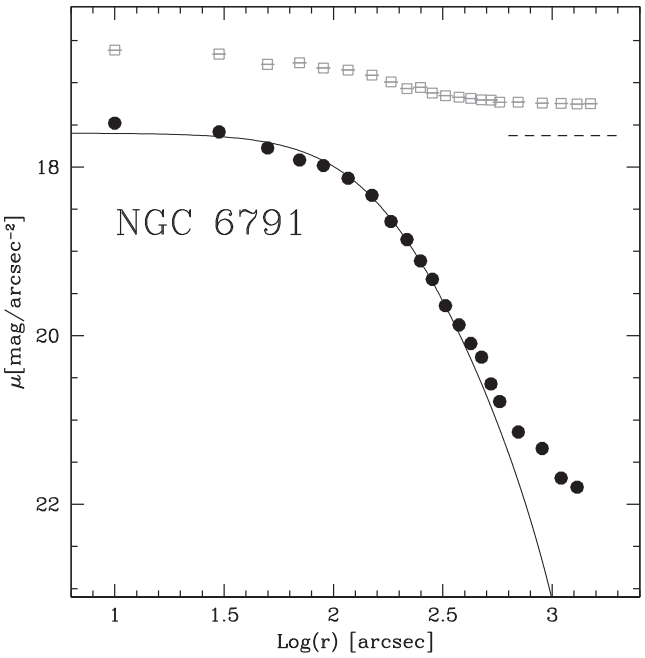

Figure 7. Optical instrumental surface brightness profile for NGC 6791.The grey empty squares represent the observed raw profile, while the black circles are the sky subtracted values. The horizontal dashed line marks the estimated of the background level as inferred in the north-west quadrant. The background-subtracted profile is shown with filled black circles.

It is worth noting that King et al. (2005) observed a rather flat mass function in the centre of NGC 6791 by using very deep *Hubble Space Telescope* observations. This observational evidence further supports the results obtained in this work. In fact, for clusters that experienced episodes of mass-loss, a flat mass function is expected because of the preferential depletion of low-mass stars. A detailed analysis of the radial variation of the mass function of this system will be presented in an upcoming paper (Dalessandro et al., in preparation).

5 MASS-LOSS AND INITIAL MASS ESTIMATE

The observational evidence presented in the previous sections reveal that NGC 6791 might have lost a fraction of its original mass due to environmental effects (like tidal shocks due to close interactions with giant molecular clouds, spiral arms, the Galactic disc and, in general, to the interactions with the Galactic tidal field) or internal dynamical effects (like two-body relaxation). In this section, we attempt to estimate the total mass lost by NGC 6791 during its evolution and derive its original mass.

While many recipes can be used for this purpose (e.g. Vesperini et al. 2013), we adopted the approach described by Lamers et al. (2005). It has the advantage of describing the way the mass of a cluster decreases with time by means of relatively simple analytic expressions. The analysis by Lamers et al. (2005) accounts for the effect of both stellar and dynamical evolution. It is important to note that the results obtained with this simplified approach are in good agreement with those obtained by detailed *N*-body simulations for clusters in the tidal field of the Galaxy (see also Lamers & Gieles 2006).

Lamers et al. (2005) provide an expression for the initial mass of the cluster, $M_{\rm ini}$, in terms of its age (t) and present mass (M):

$$M_{\rm ini} \simeq \left[\left(\frac{M}{\rm M_\odot}\right)^{\gamma} + \frac{\gamma t}{t_0}\right]^{1/\gamma} [1 - q_{\rm ev}(t)]^{-1}\,, \qquad (1)$$

where t_0 is the dissolution time-scale parameter. It is a constant depending on the strength of the tidal field and it basically describes the mass-loss due to dissolution processes such as Galactic tidal field interactions and shocks due to encounters with giant molecular clouds or spiral arms (Gieles et al. 2006; Gieles, Athanassoula & Portegies Zwart 2007). The smaller values of t_0 are typically associated with encounters with molecular clouds and spiral arms, while the larger to the Galactic tidal field. Also, the longer t_0, the weaker the tidal effect is. We used $t_0 = 3.3^{+1.4}_{-1.0}$ Myr (corresponding to the disruption time of 1.3 ± 0.5 Gyr for a cluster with the initial mass of 10^4 $\rm M_\odot$), obtained by Lamers et al. (2005) by comparing the distribution of mass and age of OCs in the solar neighbourhood with theoretical predictions. This choice is reasonable since the current Galactocentric distance of NGC 6791 roughly corresponds to that of the Sun.

γ is a dimensionless index, which depends on the cluster initial density distribution and has typical values ranging from about 0.6 to 0.8, which increases with the concentration, as constrained from theoretical studies (Gieles et al. 2004) and observations (Boutloukos & Lamers 2003). γ is usually constrained by the King dimensionless potential W_0, which characterizes the concentration of the King models (King 1966). We adopted here $\gamma = 0.62$ corresponding to $W_0 = 5$ that is a typical value for OCs and is in agreement with what derived by the analysis of the observed star count density and surface brightness profiles ($W_0 = 5.3 \pm 1.0$; Section 4). However, it is important to note that the star cluster density distributions change with time, therefore including the present-day value of W_0 in equation (1) represents a crude approximation. In particular, it is well known (e.g. Trenti, Vesperini & Pasquato 2010) that the concentration of stellar systems tend to increase (and W_0 accordingly increases) as the dynamical evolution of star cluster proceeds. As a consequence, given the proportionality linking γ to W_0, if the adopted value of W_0 is larger that its initial one, also the adopted value of γ will represent an upper limit to the correct one.

The function $q_{\rm ev}(t)$ describes the mass-loss due to stellar evolution and can be approximated by the following analytical formula:

$$\log_{10} q_{\rm ev}(t) = (\log_{10} t - a)^b + c, \quad \text{for } t > 12.5\,\text{Myr}, \qquad (2)$$

where a, b and c are coefficients that depend on the cluster metallicity. The [Fe/H] abundance of NGC 6791 is about +0.4 ($Z \sim 0.05$; Carraro et al. 2006, Gratton et al. 2006, Origlia et al. 2006) leading (see table 1 and equation 2 by Lamers et al. 2005) to values of $a = 7.00$, $b = 0.25$ and $c = -1.82$.

Equation (1) depends also on the cluster current mass M and its current age t. We adopted a current mass $M = 5000\,\rm M_\odot$ as derived by Platais et al. (2011) and age $t = 8$ Gyr (Grundahl et al. 2008, García-Berro et al. 2010, Brogaard et al. 2012). These values possess significant errors and their exact estimate is still a matter of debate; however, it is important to note that the final error in the initial mass estimate is driven mostly by the uncertainty in the dissolution time-scale parameter t_0. The dependence of the cluster initial mass on t_0 within the range of $3.3^{+1.4}_{-1.0}$ Myr is plotted in Fig. 8, together with the spread caused by the uncertainty of the current cluster mass (lower and upper limit of 4000 and 6000 $\rm M_\odot$ considered) and its current age (lower and upper limit of 7 and 9 Gyr considered).

The initial mass of NGC 6791 obtained by equation (1) turns out to be $M_{\rm ini} = (1.5\text{–}4) \times 10^5\,\rm M_\odot$, i.e. more than 50 times larger than its present-day mass. For reasonable smaller values of W_0,[3] the initial mass derived by means of equation (1) will be slightly larger, but still compatible within the errors with the value quoted above.

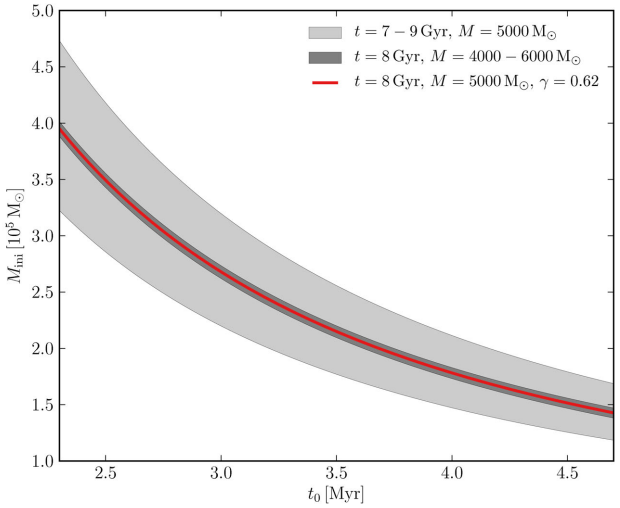

Figure 8. Cluster initial mass given by equation (1) as a function of the dissolution time-scale parameter t_0. The red curve shows the dependence derived for the current cluster mass of 5000 $\rm M_\odot$ and its age of 8 Gyr; the dark-grey coloured area corresponds to values derived for mass within 4000–6000 $\rm M_\odot$ at age of 8 Gyr; the light-grey area corresponds to values derived for the mass of 5000 $\rm M_\odot$ at an age within 7–9 Gyr.

It is important to stress that this estimate is based on a simplified approach and on parameters derived by the average behaviours of OCs. Different recipes and assumptions may likely lead to slightly different results.

6 CONCLUSIONS

In this study, we have presented a deep, wide field, photometric data set extending well beyond the tidal radius of the massive OC NGC 6791. This data set allowed us to derive updated estimates of its structural parameters, by fitting a King profile over both the star counts and surface brightness profiles. With respect to previous studies, that were limited in spatial coverage (Platais et al. 2011), the King model best fit the projected density profile turns out to have larger values of both c and $r_{\rm t}$.

More interestingly, for the first time, we detected clear signatures of tidal features in the star distribution of NGC 6791, in the form of irregular, but evident, elongation and tidal tails. Some of them seem to closely follow the cluster motion, while others are nearly perpendicular to the Galactic disc. These are clearly visible both in the 2D surface density map and in the projected density profile and they represent typical evidence of recent stellar mass-loss. We can therefore argue that NGC 6791 might have lost quite a significant fraction of its original mass while orbiting around the Galactic Centre. By using a simple analytic approach (Lamers et al. 2005), we estimated the mass likely lost by NGC 6791 during its evolution because of the effect of both stellar evolution and dynamical interactions. From this calculation, we estimated the mass at its birth to

[3] Note that OCs with very small values of the dimensionless potential ($W_0 < 3$), are expected to be completely destroyed in a short time-scale ($\sim 10^7$ yr).

be $M_{\rm ini} = (1.5–4) \times 10^5$ M$_\odot$, several tens larger than its present-day mass.

This derivation lends support to a scenario in which NGC 6791 was a much more massive system. This would qualitatively explain why the cluster could have survived for such a long-time (its age is around 7–8 Gyr) contrary to the expectations of current estimates for the destruction rates of OCs in the Galaxy.

It is interesting to note also that $M_{\rm ini}$ is comparable to the present-day mass of most Galactic globular clusters and it can be in rough agreement with the initial mass of the least massive ones (see for example Dalessandro et al. 2014) hosting multiple stellar populations. Therefore, the estimate of $M_{\rm ini}$ obtained in this paper might set interesting constraints on the initial conditions of stellar systems able to form multiple stellar populations.

ACKNOWLEDGEMENTS

ED thanks Michele Bellazzini for useful discussions and suggestions. The authors thank the anonymous referee for the careful reading of the paper and his/her suggestions.

REFERENCES

Abazajian K. N. et al., 2009, ApJS, 182, 543
Bedin L. R., Piotto G., Carraro G., King I. R., Anderson J., 2006, A&A, 460, L27
Bensby T. et al., 2013, A&A, 549, A147
Bergond G., Leon S., Guibert J., 2001, A&A, 377, 462
Binney J., Tremaine S., 1987, Galactic Dynamics. Princeton Univ. Press, Princeton, NJ, p. 747
Boutloukos S. G., Lamers H. J. G. L. M., 2003, MNRAS, 338, 717
Bragaglia A., Sneden C., Carretta E., Gratton R. G., Lucatello S., Bernath P. F., Brooke J. S. A., Ram R. S., 2014, ApJ, 796, 68
Brogaard K. et al., 2012, A&A, 543, A106
Buzzoni A., Bertone E., Carraro G., Buson L., 2012, ApJ, 749, 35
Capuzzo-Dolcetta R., Di Matteo P., Miocchi P., 2005, AJ, 129, 1906
Carraro G., 2014, in Lee H.-W., Kang Y. W., Leung K.-C., eds, ASP Conf. Ser. Vol. 482, The Tenth Pacific Rim Conference on Stellar Astrophysics. Astron. Soc. Pac., San Francisco, p. 245
Carraro G., Villanova S., Demarque P., McSwain M. V., Piotto G., Bedin L. R., 2006, ApJ, 643, 1151
Combes F., Leon S., Meylan G., 1999, A&A, 352, 149
Cunha K. et al., 2015, ApJ, 798, L41
Dalessandro E., Beccari G., Lanzoni B., Ferraro F. R., Schiavon R., Rood R. T., 2009, ApJS, 182, 509
Dalessandro E., Schiavon R. P., Rood R. T., Ferraro F. R., Sohn S. T., Lanzoni B., O'Connell R. W., 2012, AJ, 144, 126
Dalessandro E. et al., 2013, ApJ, 778, 135
Dalessandro E. et al., 2014, ApJ, 791, L4
Davenport J. R. A., Sandquist E. L., 2010, ApJ, 711, 559
García-Berro E. et al., 2010, Nature, 465, 194
Geisler D., Villanova S., Carraro G., Pilachowski C., Cummings J., Johnson C. I., Bresolin F., 2012, ApJ, 756, L40
Gieles M., Baumgardt H., Bastian N., Lamers H. J. G. L. M., 2004, in Lamers H.J.G.L.M., Smith L.J., Nota A., eds, ASP Conf. Ser. Vol. 322, The Formation and Evolution of Massive Young Star Clusters. Astron. Soc. Pac., San Francisco, p. 481
Gieles M., Portegies Zwart S. F., Baumgardt H., Athanassoula E., Lamers H. J. G. L. M., Sipior M., Leenaarts J., 2006, MNRAS, 371, 793
Gieles M., Athanassoula E., Portegies Zwart S. F., 2007, MNRAS, 376, 809
Gieles M., Baumgardt H., 2008, MNRAS, 389L, 28
Gratton R., Bragaglia A., Carretta E., Tosi M., 2006, ApJ, 642, 462
Gratton R. G., Carretta E., Bragaglia A., 2012, A&ARv, 20, 50
Grundahl F., Clausen J. V., Hardis S., Frandsen S., 2008, A&A, 492, 171
Jílková L., Carraro G., Jungwiert B., Minchev I., 2012, A&A, 541, A64
Johnston K. V., Zhao H., Spergel D. N., Hernquist L., 1999, ApJ, 512, L109
King I. R., 1966, AJ, 71, 64
King I. R., Bedin L. R., Piotto G., Cassisi S., Anderson J., 2005, AJ, 130, 626
Kuhn J. R., Smith H. A., Hawley S. L., 1996, ApJ, 469, L93
Küpper A. H. W., Kroupa P., Baumgardt H., Heggie D. C., 2010, MNRAS, 407, 2241
Lamers H. J. G. L. M., Gieles M., 2006, A&A, 455, 17
Lamers H. J. G. L. M., Gieles M., Bastian N., Baumgardt H., Kharchenko N. V., Portegies Zwart S., 2005, A&A, 441, 117
Leon S., 1998, PhD thesis Univ. Paris 7, France
Liebert J., Saffer R. A., Green E. M., 1994, AJ, 107, 1408
Miocchi P. et al., 2013, ApJ, 774, 151
Montuori M., Capuzzo-Dolcetta R., Di Matteo P., Lepinette A., Miocchi P., 2007, ApJ, 659, 1212
Odenkirchen M. et al., 2001, ApJ, 548, L165
Odenkirchen M. et al., 2003, AJ, 126, 2385
Origlia L., Valenti E., Rich R. M., Ferraro F. R., 2006, ApJ, 646, 499
Platais I., Cudworth K. M., Kozhurina-Platais V., McLaughlin D. E., Meibom S., Veillet C., 2011, ApJ, 733, L1
Rockosi C. M. et al., 2002, AJ, 124, 349
Sollima A., Martínez-Delgado D., Valls-Gabaud D., Peñarrubia J., 2011, ApJ, 726, 47
Spitzer L., Jr, 1958, ApJ, 127, 17
Spitzer L., Jr, Harm R., 1958, ApJ, 127, 544
Stetson P. B., 1987, PASP, 99, 191
Tofflemire B. M., Gosnell N. M., Mathieu R. D., Platais I., 2014, AJ, 148, 61
Trenti M., Vesperini E., Pasquato M., 2010, ApJ, 708, 1598
Vesperini E., McMillan S. L. W., D'Antona F., D'Ercole A., 2013, MNRAS, 429, 1913
Wilson C. P., 1975, AJ, 80, 175

This paper has been typeset from a TEX/LATEX file prepared by the author.